Frequency shifts in injection-seeded optical parametric oscillators with phase mismatch

T. D. Raymond, W. J. Alford, and A. V. Smith

Sandia National Laboratories, Albuquerque, New Mexico 87185-0601

Mark S. Bowers

Aculight Corporation, Bellevue, Washington 98005

Received February 28, 1994

We have observed a frequency shift in the output signal pulses relative to the seed frequency in an injection-seeded, singly resonant, critically phase-matched, pulsed optical parametric oscillator in which phase mismatch was intentionally introduced. The observed shifts can be large compared with the linewidth of the signal pulse, are approximately linear in phase mismatch, and increase with increasing pump fluence. We observe frequency shifts of as much as ±400 MHz for our 532-nm-pumped, potassium titanyl phosphate ring optical parametric oscillator. For zero phase mismatch, we observe nearly transform-limited linewidths of less than 130 MHz. We compare the experimental data to a simple analytic model that overestimates the shifts because it ignores pump depletion. We also compare our measurements with a numerical model that calculates the two-dimensional, transient electric fields and the resultant spectral distributions while explicitly including walk-off, diffraction, and pump depletion. We find good agreement between the experimental data and the results of this model.

Singly resonant optical parametric oscillators (OPO's) with their broad tunability are promising sources for spectroscopic applications because they can be easily tuned to atomic and molecular absorptions. Unfortunately, the linewidths of pulsed OPO's are generally much broader than most Doppler- and pressure-broadened transitions. Narrower OPO linewidths can be obtained by dispersive elements in the cavity[1] or by injection seeding.[2–9] If a seed source is available, injection seeding with a low-power, narrow-bandwidth source permits simple cavity designs and provides single-longitudinal-mode output in pulsed OPO's. Injection seeding also reduces the OPO threshold and improves the OPO efficiency, in part by reducing the OPO buildup time.

For applications in which precise frequency control is required, it is necessary to understand the mechanisms that affect the output frequency of injection-seeded OPO's. As with injection-seeded lasers,[10] detuning between the seed frequency and the closest power oscillator cavity resonance can lead to frequency shifts in the OPO output. When the cavity is resonant with the injected signal seed wave, additional mechanisms can lead to a frequency shift between the injected signal and the signal output of a pulsed singly resonant OPO[4]: phase mismatch, nonresonant idler feedback, and nonlinear index of refraction. Each of these mechanisms impresses phase shifts upon the waves interacting with the crystal. Because the resonated wave experiences this phase shift, $\Delta\phi$, on each round trip, its frequency is shifted by approximately $\Delta\phi/\tau$, where τ is the cavity round-trip time.

In this Letter we focus on the effect of phase mismatch on the frequency profiles and shifts of the output signal pulse for an injection-seeded pulsed OPO under conditions in which cavity detuning, idler feedback, and nonlinear index of refraction contribute negligibly to the observed shifts. We compare experimental measurements with two models: (1) a simple analytic model that ignores pump depletion but allows simple estimates of the shifts and (2) a detailed numerical model including pump depletion, diffraction, and walk-off that calculates the time-dependent signal, idler, and pump fields and their spectral distributions.

Phase-velocity mismatch in the parametric process is defined as $\Delta kL = [k_p - (k_s + k_i)]L$, where k_p, k_s, and k_i are the pump, signal, and idler wave vectors, respectively. When phase mismatch is present in optical parametric amplification, the amplified wave experiences a phase shift because the wave vector of the polarization producing that amplification is not equal to that of the incident wave. The phase shift of the amplified wave (relative to the incident wave) increases with phase mismatch and amplification. It can be shown that in the undepleted-pump, high-gain limit[11] this shift approaches $\Delta kL/2$ with a corresponding frequency shift of $-\Delta kL/(2\tau)$.

The experimental setup is shown in Fig. 1. The pump beam is the spatially filtered 532-nm output of a frequency-doubled, Q-switched, injection-seeded Nd:YAG laser operating at 10 Hz. It is a collimated beam with a 0.6-mm FWHM and an 8-ns FWHM pulse width whose spatial and temporal profiles are well approximated by Gaussian distributions. The peak pump fluence is limited to 2.5 J/cm^2 (300 MW/cm^2) to prevent damage to the optics and potassium titanyl phosphate (KTP) crystal. At this peak pump intensity we estimate that shifts that are due to nonlinear index of refraction, n_2, are less than 15 MHz for $\Delta kL = 0$ from the value measured

0146-9592/94/191520-03$6.00/0

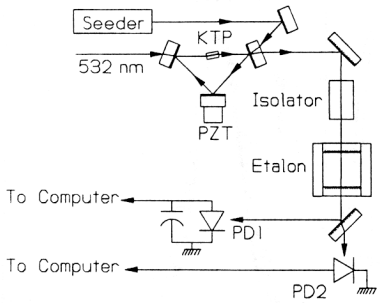

Fig. 1. Experimental layout: the seed and pulsed signal outputs from the OPO are analyzed with a high-finesse étalon. Photodiode PD1 is sensitive primarily to the seed beam, and photodiode PD2 detects the pulsed signal beam from the OPO. PZT, piezoelectric transducer.

by DeSalvo *et al.*[12] for KTP. We ignore n_2 effects in the models.

The OPO is a singly resonant, three-mirror (flat–flat–flat) ring cavity similar to that used by Hamilton and Bosenberg.[8] It consists of two 780-nm high reflectors and a 780-nm 51% reflective output coupler. This cavity resonates the signal wave at 780 nm but provides less than 0.1% feedback of the 1.67-μm idler and 532-nm pump waves to minimize the effects of idler and pump feedback on the signal frequency. We estimate that frequency shifts that are due to idler feedback are only a few megahertz for our conditions. The cavity length is 6.7 cm, yielding a cavity mode spacing of 4.0 GHz. The KTP crystal is cut for critical phase matching ($\theta = 51°$, $\phi = 0°$) and is antireflection coated for 780 and 532 nm. The signal wave is an extraordinary wave polarized in the plane of the cavity experiencing a walk-off of 0.52 mm relative to the pump and idler waves in the 1-cm-long crystal. The pump and idler waves are ordinary waves polarized out of the plane of the ring. The seed and pump beams are aligned to within 0.5 mrad of the cavity optic axis for collinear phase matching. The phase mismatch is approximately linear with the external crystal angle for the small range of angles investigated here, i.e., $\Delta kL = (-4 \times 10^3/\text{rad})(\theta - \theta_0)$, where θ is the external crystal angle and θ_0 is the external phase-match angle. Precise determination of θ_0 is difficult when one is simply optimizing the energy output of the OPO; hence we have arbitrarily defined θ_0 to be that crystal angle for which there is zero frequency shift between the output signal and seed beams when the seeded OPO is operating near threshold (0.66 J/cm^2). At higher pump fluence there is a small shift in the signal frequency at this angle.

We use a single-frequency (<30 MHz FWHM) cw titanium-doped sapphire laser to injection seed the OPO through the output coupler. Typically the seed beam contains 30–40 mW of power in a beam slightly larger than the pump beam. One of the high-reflectivity mirrors, mounted on a piezoelectric transducer, permits fine adjustment of the cavity length. The OPO cavity is locked to the seed frequency by a standard modulation technique. To prevent frequency jitter that results from the dither in the cavity length imposed by this technique, we fire the Nd:YAG laser when the cavity is precisely resonant with the seed.[4] The cavity is thus kept resonant with the seed frequency to within ±15 MHz.

The seed beam and the pulsed signal beam from the OPO are expanded, collimated, and spectrally resolved with a high-finesse (>60) scanning Fabry–Perot étalon of 974-MHz free spectral range. An optical isolator located between the OPO and the étalon prevents feedback into the OPO and the seed laser. The transmitted seed power is detected 1 ms before the pump laser fires with an electrically filtered photodiode (PD1), sensitive primarily to cw signals. The much more intense output signal pulse is detected with a fast photodiode (PD2). To obtain the spectra, we slowly scan the étalon while the transmitted seed power and the OPO signal energy are simultaneously recorded with a computer.

Figure 2 shows the measured and calculated frequency shift, $\delta\nu = \nu_{\text{signal}} - \nu_{\text{seed}}$, where ν_{signal} is the peak of the output signal pulse spectral distribution and ν_{seed} is the seed frequency, for peak pump fluences of 1.6 and 2.5 J/cm^2 as a function of ΔkL. The range in the horizontal axis in these graphs corresponds to a total excursion of ±1 mrad (0.06°) in the external crystal angle. The observed shifts are nearly linear in phase mismatch and have best-fit slopes of −90 and −30 MHz/rad for 1.6- and 2.5-J/cm^2 peak pump fluences, respectively. We have observed shifts of as much as ±400 MHz from the seed frequency.

The dashed curves in Fig. 2 are the signal frequency shift (signal phase shift divided by the cavity round-trip time) calculated with the undepleted-pump, steady-state solutions to the three coupled-wave equations[11] averaged over the signal intensity. We assume that a signal seed, Gaussian in space, is amplified in a crystal pumped by a Gaussian beam in time and space. Note that this frequency shift is not simply the high-gain limit, $-\Delta kL/(2\tau)$. This simple model qualitatively predicts the pump dependence, magnitude, and sign of

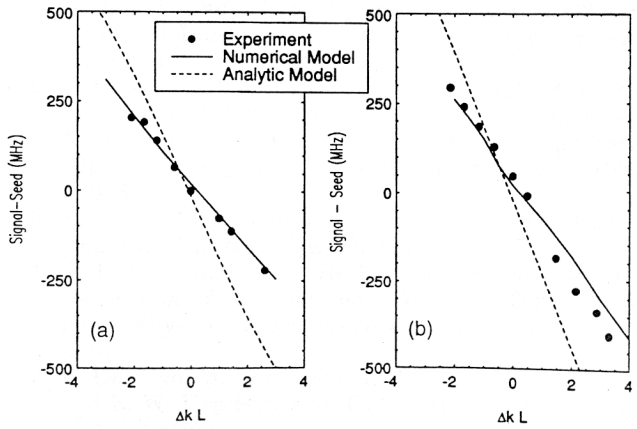

Fig. 2. Experimentally measured frequency shifts (filled circles) as a function of phase mismatch for peak pump fluences of (a) 1.6 J/cm^2 and (b) 2.5 J/cm^2. The solid curves represent the shifts calculated with the numerical model described in the text, and the dashed curves represent the shifts calculated with the analytic model.

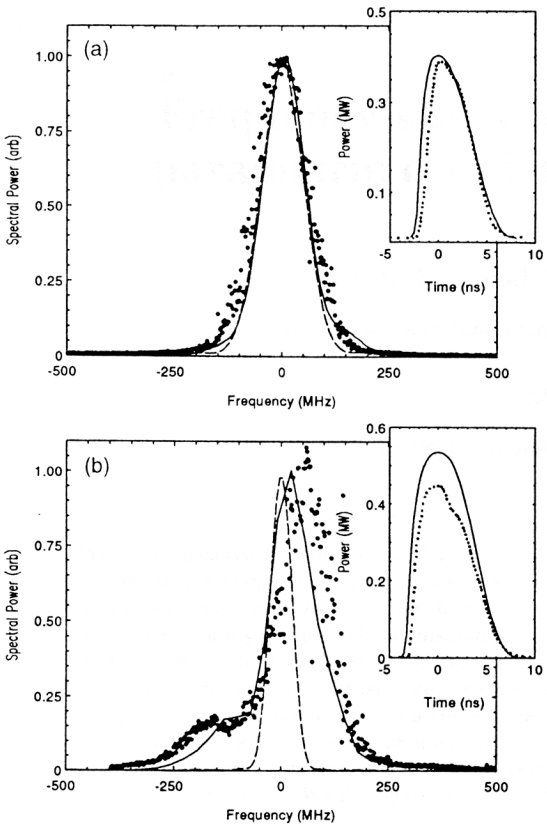

Fig. 3. Spectral and temporal (insets) profiles for the output signal pulse when $\Delta kL = 0$ and the peak pump fluence is (a) 1.6 J/cm^2 and (b) 2.5 J/cm^2. The dots are experimentally measured results, the solid curves are results from the numerical model, and the dashed curves are transforms of the temporal data assuming a constant phase.

the shift but overestimates the shift as a function of ΔkL because the undepleted-pump approximation is violated in actual OPO operation.

The solid curves in Fig. 2 represent the calculated shifts for the output signal pulse with a model[13] that integrates the three coupled-wave equations,[11] including pump depletion, walk-off, and diffraction in the paraxial approximation. The incident pump field is taken to be Gaussian in space and time. The time-dependent two-dimensional electric fields of the signal, idler, and transmitted pump waves are computed by propagation of time slices out of each wave through the nonlinear crystal and around the ring. A time slice for each wave is equal to the cavity round-trip time (0.25 ns). The temporal Fourier transform of the fields yields the power spectrum of each wave.

Figures 3 shows the calculated (solid curves) and measured (dots) spectral and temporal profiles for the signal beam when $\Delta kL = 0$ for peak pump fluences of 1.6 J/cm^2 (2.4 times threshold) and 2.5 J/cm^2 (3.8 times threshold). At 1.6 J/cm^2 the measured spectral profile has a 127-MHz FWHM that is nearly equal to the 115-MHz FWHM of the transform of the 4.8-ns FWHM temporal profile assuming a constant phase and in good agreement with the 120-MHz FWHM predicted by the numerical model. This measurement suggests that there is little time dependence in the phase during the pulse.

At 2.5 J/cm^2 the measured spectral profile has a FWHM of 125 MHz, is shifted by +60 MHz, and is skewed toward zero frequency shift, indicating the presence of time-dependent structure on the signal phase. The numerical model accurately predicts a spectral profile with a FWHM of 119 MHz and a small shoulder on the low-frequency side. The model does predict the observed asymmetry and the shoulder on the low-frequency side, but it predicts a shift of only +22 MHz.

In summary, we have observed a shift in the frequency of the output signal pulse of an injection-seeded pulsed OPO relative to the seed beam when phase mismatch is present. The shift is approximately linear in phase mismatch and increases with increasing pump fluence. The observed line shapes are nearly transform limited at low pump fluences and show evidence of time-dependent phase variations at high pump fluences. We have developed a numerical model including pump depletion, diffraction, and walk-off that accurately predicts the observed frequency shifts as well as the temporal and spectral profiles.

This research was supported by the U.S. Department of Energy under contract DE-AC04-94AL85000.

References

1. S. J. Brosnan and R. L. Byer, IEEE J. Quantum Electron. **QE-15,** 415 (1979).
2. J. E. Bjorkholm and H. G. Danielmeyer, Appl. Phys. Lett. **15,** 171 (1969).
3. Y. X. Fan, R. C. Eckardt, R. L. Byer, J. Nolting, and R. Wallenstein, Appl. Phys. Lett. **53,** 2014 (1988).
4. D. C. Hovde, J. H. Timmermans, G. Scoles, and K. K. Lehmann, Opt. Commun. **86,** 294 (1991).
5. F. Huisken, A. Kulcke, D. Voelkel, C. Laush, and J. M. Lisy, Appl. Phys. Lett. **62,** 805 (1993).
6. N. P. Barnes, K. E. Murray, and G. H. Watson, in *Advanced Solid-State Lasers,* L. L. Chase and A. A. Pinto, eds., Vol. 13 of OSA Proceedings Series (Optical Society of America, Washington, D.C., 1992), p. 356.
7. J. G. Haub, M. J Johnson, B. J. Orr, and R. Wallenstein, Appl. Phys. Lett. **58,** 1718 (1991).
8. C. E. Hamilton and W. R. Bosenberg, in *Conference on Lasers and Electro-Optics,* Vol. 12 of 1992 OSA Technical Digest Series (Optical Society of America, Washington, D.C., 1992), p. 370.
9. L. R. Marshall, A. Kaz, O. Aytur, and R. L. Burnham, in *Advanced Solid-State Lasers,* L. L. Chase and A. A. Pinto, eds., Vol. 13 of OSA Proceedings Series (Optical Society of America, Washington, D.C., 1992), p. 338.
10. Y. K. Park, G. Giuliani, and R. L. Byer, IEEE J. Quantum Electron. **QE-20,** 117 (1984).
11. R. L. Byer and R. L. Herbst, in *Nonlinear Infrared Generation,* Y.-R. Shen, ed., Vol. 16 of Topics in Applied Physics (Springer-Verlag, New York, 1977), p. 97.
12. R. DeSalvo, M. Sheik-Bahae, A. A. Said, D. J. Hagan, and E. W. Van Stryland, Opt. Lett. **18,** 194 (1993).
13. M. S. Bowers and A. V. Smith, in *Advanced Solid-State Lasers,* T. Y. Fan and B. H. T. Chai, eds., Vol. 20 of OSA Proceedings Series (Optical Society of America, Washington, D.C., 1994), p. 471.